

# Real-time anchor node selection for two-way-ranging (TWR) ultra-wideband (UWB) indoor positioning systems

Ben Van Herbruggen<sup>1</sup>, Dries Van Leemput<sup>1</sup>, Jaro Van Landschoot<sup>1</sup> and Eli De Poorter<sup>1</sup>

<sup>1</sup>IDLab, Department of Information Technology at Ghent University - imec

Manuscript received June XXX.XX; revised XXX.XX; accepted July XXX.XX. Date of publication XXX.XX; date of current version XXX.XX.

**Abstract**—The progress in cm-accurate ultra-wideband (UWB) localization systems encourages the adoption on larger scales. To calculate the distance between a mobile tag and anchor nodes with known locations, a two-way-ranging (TWR) scheme is often used where the time-of-flight (TOF) is determined by exchanging at least two packets. This TWR scheme avoids the need for synchronization between devices to compensate for clock drift. However, in TWR systems, mobile tags continuously need to decide with which anchor nodes to range. Currently, most scientific papers assume the tag ranges sequentially with all anchor nodes, thereby limiting the scalability. In addition, precious time is wasted trying to range with anchors that encounter poor channel characteristics. This paper proposes two novel anchor selection algorithms that tackle both problems. Anchors are selected in real-time based on their link quality, improving accuracy by selecting the best-performing anchor nodes. The algorithms are based on heuristic methods to estimate the link quality and the corresponding ranging error. The algorithm's two variants are evaluated in a realistic dynamic industrial setup, reaching an accuracy up to 15 cm. This represents a 50% improvement compared to ranging with all available anchors.

**Index Terms**—Indoor positioning system (IPS), Ultra-Wideband (UWB), anchor selection, Industry 4.0, Two Way Ranging (TWR)

## I. INTRODUCTION

Indoor positioning systems (IPSs) are deployed in many different domains for optimizing industrial processes and consumers comfort [1]–[3]. Due to the variability in environments and requirements (e.g., accuracy, latency, cost, and hardware availability), many different technologies are used for these systems: vision-based, lidar, RF time-of-flight (TOF), etc. A popular technology is ultra-wideband (UWB) due to its large bandwidth, resulting in low transmission power values, high penetration capabilities, and robustness against multi-path degradation [4]. In addition, the excellent time resolution of UWB permits the use of TOF techniques to estimate the localization of a mobile tag with cm-level precision. This TOF and corresponding distance is often determined with the two-way-ranging (TWR) localization scheme. In TWR, devices send two or three packets back and forth to measure the distance between sender and receiver. This scheme does not require clock synchronization between the anchors, making it a suitable candidate for large-scale, multi-room localization systems. However, scaling this approach towards deployments with tens or hundreds of anchor devices requires real-time anchor selection to obtain a high positioning update rate and accuracy. In contrast, an alternative time-based method for localization is time-difference-of-arrival (TDoA), which estimates the position of a mobile tag based on a single UWB packet by using the arrival delays on all clock-synchronized anchor nodes within reach. For TDoA localization systems, various anchor selection approaches have been presented [5]–[7]. However, in TDoA systems, there is no need for dynamically discovering and communicating with a subset of anchor nodes since the anchors are only receiving.

The main contributions of this paper are as follows: i) We propose two novel anchor selection methods for TWR localization, one that is compatible with a default MAC protocol that ranges with all anchor nodes and one that adjusts the behavior to dynamically select and

communicate with a subset of anchor nodes and ii) We evaluate the proposed algorithms in a realistic industrial environment and compare them to state-of-the-art approaches. To the best of our knowledge, we are the first to evaluate both approaches with a real-time dynamic trajectory in an industrial environment and to compare them to reference scenarios.

The remainder of this paper has the following structure: Section II discusses prior work on anchor selection for UWB. In Section III, a link quality factor is discussed. The proposed algorithms that use these metrics are introduced in Section IV. Section V then gives an overview of how data is measured and collected in our IIoT lab [8], alongside the localization algorithm. The evaluation of the proposed algorithms is given in Section VI. Section VII concludes this paper.

## II. RELATED WORK

This section discusses relevant state-of-the-art (SOTA) algorithms on anchor selection. Details of the relevant work are given in Table 1. There is currently only a limited number of anchor selection algorithms for TWR UWB localization systems.

Therefore, the anchor node selection algorithms for TWR can be divided into two different approaches: a global and a local approach. The global approach uses the original medium access control where the tag schedules to range with all anchors. Afterward, the positioning is calculated based on a subset of these anchors. This approach increases the accuracy by removing unreliable ranges but still limits the scalability and update rate of the system. The local approach continuously identifies the best anchor nodes to range with and ranges only with those anchor nodes. This approach is more scalable in terms of update rate and energy consumption. However, as the tag is only ranging with a selected set of anchor nodes, it cannot take the link quality of other anchor nodes into account.

First, related work for the global discovery approach is discussed, whereby the mobile tag always ranges with all anchor nodes and then selects a subset of these measurements to calculate the position. In [9]

Table 1: Comparison of the proposed algorithm to state-of-the-art anchor selection algorithms.

	approach	Algorithmic			Evaluation				
		DOP	link metrics	NLOS	area	Scale (# of anchors)	test scenario	accuracy improvement	
state-of-the-art	Chen et al [9]	global	-	3	yes	14x14 m <sup>2</sup>	6	static (12 points)	40%
	Courtay et al [10]	global	-	-	yes	26.4x9 m <sup>2</sup>	6	-	-
	Djosic et al [11]	global	-	-	yes	80 m <sup>2</sup>	6	static (720 points)	-
	De Cock et al [12]	global	-	yes	yes	6.3x4.4 m <sup>2</sup>	8	-	-
	Motroni et al [2]	local	yes	-	-	40x25 m <sup>2</sup>	35	-	-
	Jimenez et al [13]	local	yes	-	yes	80 m <sup>2</sup>	2 × 4	-	-
proposed	non-constrained	global	yes	3	yes	30x10 m <sup>2</sup>	23	25m trajectory	49%
	on-tag	local	-	3	yes	30x10 m <sup>2</sup>	23	25m trajectory	31%

three metrics of the UWB link are used to determine its quality: 1) the channel factor which represents the similarity between the received and ideal channel impulse response (CIR), 2) the power ratio between the full packet and the first path and 3) the time difference between the first and the highest peak. The positioning algorithm then selects the four anchors with the best link quality. If one of these anchors does not meet the quality threshold, the algorithm instead selects the closest anchor nodes. Similar to this work, our approach also uses link metrics, but we don't require any CIR collection and extract them by directly accessing the registers of the DW1000, making our approach computationally more efficient. A second example is [10], where the best anchor selection for trilateration (BAST) algorithm has been proposed, predicting the position based on the two previous positions. Afterward, it selects the set of three anchors closest to this predicted value. However, in contrast to our work, no link quality is taken into account. The BAST algorithm can achieve up to 4.17 times better accuracy compared to weighted centroid localization and 1.26 times better than multilateration. In [11], a database with distances to 11 temporary anchor nodes is constructed during the deployment of the system. Depending on the zone of the mobile node estimated by the six fixed anchors, line-of-sight (LOS) distances from the database are injected into the system to improve localization accuracy. A final example of anchor selection is [12], where different anchor nodes are selected based on the first path of the signal when human body shadowing is present. For this method, a mean improvement of 27% is achieved. The results can be improved when inertial measurement unit (IMU) is added to select anchor nodes.

To the best of our knowledge, only a single implementation exists that implements a local discovery approach, whereby nearby nodes are dynamically discovered rather than ranging with all anchor nodes: the commercial-of-the-shelf MDEK1000 evaluation kit. The kit consists of boards with the DW1000 UWB radio and supporting closed-source software. The tag will first estimate its location, after which it will select one anchor node in each quadrant to range with [14]. Although the tag ranges with a maximum of four anchors, all anchor coordinates in the whole system should be known to the tag, limiting its usefulness in unknown environments. In addition, the kit is closed-source and lacks the necessary information and flexibility to make changes to the protocols [13]. In [2], this evaluation kit was used, where it was concluded that the system performance degrades significantly in difficult non-line-of-sight (NLOS) situations. Finally, as shown in Table 1, in contrast to our work, most existing publications are severely limited in that they are only evaluated in a small environment with a limited number of anchor nodes (typically around six) and no dynamic moving mobile node. As such, there is a clear need for alternative local-discovery approaches that are scientifically described, include more advanced link metrics, and are evaluated more thoroughly.

### III. LINK AND LOCALIZATION METRICS

The first important criterion to select which anchor nodes to use is the estimation of the quality  $Q$  of an UWB link, allowing to detect links with higher ranging error probabilities. Our quality metric is based on three different properties of the received signal: received power, the power ratio between the first path power in the CIR and the total received power, and the peak distance in time between the first and highest peak in the CIR. The choice for these metrics is based on published research on the link quality [9], [12], [15], [16], which shows a low value of these metrics indicates higher link quality. As a first indicator, the **received power** ( $P_{rx}$ ) is reported by the DW1000 [16] which is inversely proportional to the squared traveled distance [17]. NLOS reflections cause a lower received power due to attenuation along the direct path or longer reflected paths, leading to a higher error probability. The contribution of  $P_{rx}$  is the difference between the actual received power and high received power (-80 dBm), with lower values indicating a better link. Second, the **power ratio** ( $P_{ratio}$ ) between the first path power and the total received power is an indicator of NLOS behavior, as the first path contains the majority of the power in LOS conditions. Third, the **peak distance** ( $d_{peaks}$ ) in time between the first and highest peak gives additional information about the first path and secondary reflection peaks, as this metric will be low in optimal conditions. The further the highest peak is situated from the first, the longer the reflected path and the higher the attenuation on the first path. Fig. 1 depicts a CIR with a high reflected path, showing higher chances of NLOS in the link and indicating a lower quality. To combine these different metrics into a single link quality factor  $Q$ , the metrics are first normalized and then assigned weights based on empirical testing using multiple experimental static setups, resulting in the following relation:

$$Q = 0.6 \times P_{rx} + 0.3 \times P_{ratio} + 0.1 \times d_{peaks} \quad (1)$$

A higher score reflects a link with higher error probabilities which permits the determination of the best subset of anchors for localization. Although three distances are the minimum to locate an object in 2D, it is often beneficial to use additional anchor nodes to account for temporal signal blockage, packet loss, or poorly placed anchor nodes. As such, similar to previous TDoA work [5], [7], in our work up to five anchor nodes are selected using the quality metric factor.

Next, the selection using  $Q$  is expanded by taking the dilution of precision (DOP) of the selected anchor nodes into account. As DOP is a measure of how much the geometry will multiply the ranging errors for the localization, it affects the uncertainty of the localization accuracy. In [18], simulations proved that the errors can be reduced when selecting the best anchors based on the DOP value. However, to calculate the DOP for a certain position, the positions for both anchors and tag need to be known, which makes it challenging to deploy it in real-time on a constrained user device.

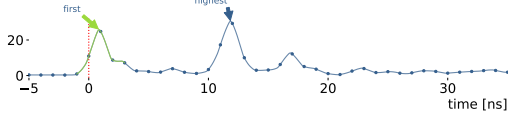


Fig. 1: The CIR is a representation of the channel centered around the first path at time 0.

#### IV. PROPOSED ANCHOR SELECTION ALGORITHMS

In this section, we propose two new anchor node selection algorithms. A non-constrained algorithm that follows the global discovery approach and a real-time embedded on-tag algorithm using the local discovery approach.

The **non-constrained algorithm** is designed to be executed on an edge node or non-constrained tag. The tag ranges sequentially with all anchors which does not yield a higher update rate but allows the localization server to exploit detailed information (e.g. received power, peak path, ...) from all anchors to perform the anchor selection. Based on the collected information, the localization server selects four anchor nodes based on their link quality  $Q$  and a fifth based on both the link quality and the DOP of the final subset. Due to the uncertainty of the tag's position and the high computational complexity of the DOP, only the last anchor is selected based on its DOP. By weighting the normalized DOP and the normalized link quality equally, it is unlikely to add an anchor with a poor link but better geometry to the subset but also select the anchor with better geometry when multiple links have equal quality.

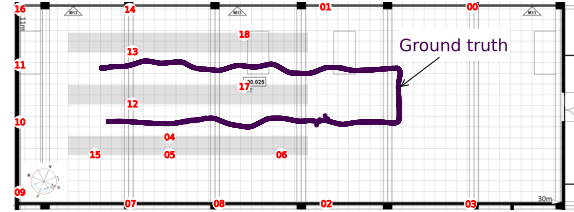
In contrast to the non-constrained algorithm, during the **proposed on-tag algorithm** the tag only ranges with a selected set of five anchor nodes. It executes the algorithm assuming constrained computational resources. As the tag is unaware of the link qualities of anchors excluding the selected set, it needs to perform the algorithm based on the information of the five selected anchor nodes. Therefore, after every range with an anchor, the link quality  $Q$  is evaluated based on a threshold  $T_{maxQ}$ . If a selected anchor fails to range or exceeds  $T_{maxQ}$  three times out of the last five ranges, the anchor is pushed out of the selected set and is blacklisted for a pre-configured duration. Then, a new anchor is selected as follows: the anchor in the selected set with the highest  $Q$  is considered, and the closest neighbor to this anchor node is added to the selection. To find an initial set of active anchors, the tag ranges with all anchors once after which the five anchors with the best link quality are chosen to start the algorithm. As a result, the tag does not need to know its position or the exact anchor coordinates, nor does it require calculating the DOP, making it a lightweight solution that can be implemented on a constrained UWB tag.

#### V. MEASUREMENT AND METHODOLOGY

The proposed algorithms are evaluated in the IIoT lab, which represents an industrial warehouse environment (see Fig. 2). The metal racks cause significant reflections and attenuation on the various links. The lab is equipped with a mm-accurate motion capturing (MOCAP) system which enables analysis of the anchor selection with both accurate ground truth and repeatable trajectories with a mobile robot. The mobile robot executes the same trajectory of 35 m at 0.14 m/s for all different algorithms. The used UWB



(a) (b)



(c)

Fig. 2: The new algorithms are evaluated (a) in the IIoTlab with (b) in total 23 Wi-Pos UWB anchors available on (c) a 35m long trajectory of the robot.

hardware consists of 23 Wi-pos nodes which combines the popular DW1000 UWB transceiver with a wireless sub-GHz backbone for communication and synchronization [19]. All UWB anchors are connected to a dedicated high-throughput cabled network to collect data from all anchor nodes without losing the update rate. Such a high-throughput network between the anchor nodes is not always feasible, motivating a lightweight anchor selection algorithm [3]. The UWB operates at channel 5 with 512 preamble symbols, 64 MHz PRF resulting in a short but stable link. In total about 7500 successful ranges were collected in the dataset. The localization server combines the distances measured with TWR and the anchor coordinates to a position estimate using a Kalman filter [20]. A Kalman filter smooths the localization points by estimating where an object is and how fast it's moving in both directions. The state vector of this Kalman filter consists of position  $(x,y)$  and velocity  $(v_x,v_y)$ . It works in two steps: 1) predicting the next state based on the previous one and uncertainties on ranging information ( $\sigma_w = 120$ ) and on the movement information ( $\sigma_v = 100$ ), and 2) updating with measurements from the UWB links. The Kalman gain, calculated with the difference between the prediction and measurement, represents measurement certainty. This, in turn, adjusts the state. Every new UWB measurement triggers both steps, updating the filter's state. The Kalman filter's only input is the UWB measurement, and it takes no input from any other sensor.

#### VI. EXPERIMENTAL EVALUATION

The performance of the proposed algorithms is compared to three alternative existing implementations: (i) **Best link selection** that has perfect information on the actual ranging error of each link<sup>1</sup>.

<sup>1</sup>In our case, the exact ranging error was calculated using mm-accurate ground truth from the MOCAP system, which is only possible if the tag's location is known with higher accuracy than the UWB system can provide

This algorithm selects the five best anchors based on the actual ranging error. Exploiting this information is not realistic in real-life deployments, and as such this algorithm can be considered as a lower bound on the achievable accuracy of the non-constrained algorithm. (ii) **Expert-based** where the tag selects a set of anchors based on expert knowledge. For every anchor, the expert determines its optimal neighbors considering LOS conditions and distance from the anchor. The tag then ranges with the neighbors of the nearest anchor. Although this scenario fully exploits human expert knowledge and limits the number of unreachable selected anchors, it requires significant manual effort and expertise to determine the neighbors of each anchor. Our proposed algorithm aims to obtain comparable performance without requiring expert intervention. (iii) An **all-anchors** algorithm that naively uses all anchors (also the ones with bad performance) to estimate the position but does not include any form of anchor selection, thereby wasting resources on unreachable anchors. This is the de-facto approach in many existing localization systems.

The update rates and errors of all algorithms are shown in Table 2. The increase in update rate allows the Kalman filter to effectively adapt to changes in the trajectory and provide a location update more frequently. As expected, the best link selection mode performs best in terms of accuracy ( $11.5 \text{ cm} \pm 4.8$ ) as it selects the links with the lowest error. The non-constrained mode ( $14.9 \text{ cm} \pm 7.1$ ) does, however, closely match this best link selection mode, indicating a good anchor selection algorithm with a rather low standard deviation. The local approach algorithms are 5 cm less accurate than the non-constrained algorithm. The two algorithms have a similar mean performance. This is because the set of selected anchors for both algorithms are quite similar although the on-tag anchor selection requires no input from an expert. However, due to monitoring of the active links, the dynamic behavior of the on-tag algorithm is more robust: the expert-based does not consider link quality or obstacles resulting in higher standard deviation. In terms of update rate, the local approach (on-tag mode and expert-based) outperforms the algorithms following the global approach by almost 2.5 times the update rate while simultaneously boosting the mean accuracy.

Table 2: Mean absolute error (MAE), standard deviation (std) and update rate for the dynamic evaluation.

		MAE [cm]	std	Update rate [Hz] per anchor
global approach	<b>All anchors</b>	29.2	22.1	0.94
	<b>non-constrained (our)</b>	14.9	7.1	0.94
	<b>best link selection</b>	11.5	4.8	0.94
local approach	<b>on-tag (our)</b>	20.2	14.8	2.28
	<b>expert-based</b>	19.5	21.8	2.28

## VII. CONCLUSIONS

The addition of anchor selection to TWR systems enhances the scalability of these systems. By limiting the number of anchors that range with the tag, we proved that both the update rate and the accuracy of the system can be improved. In this context, a quality factor for the various UWB links is proposed. This link quality factor is used as input for the proposed anchor selection algorithms. The anchor selection algorithms are categorized into two distinct approaches of which the global approach does not change the scheduling of the packets but improves positioning by selecting the best anchor nodes,

based on the link quality and DOP, from 29.2 cm to 14.9 cm. This is only 3.4 cm higher than a best link selection based on mm-accurate groundtruth. In addition to this global anchor selection algorithm, a more embedded tag-based approach is investigated, implemented, and evaluated. Although only information on the active links is present, the system reaches still an accuracy of 20.2 cm. By not scheduling ranging with unreachable anchors, the update rate is increased by 238%: from 0.94 Hz up to 2.24 Hz per anchor.

## REFERENCES

- [1] A. Frankó, G. Vida, and P. Varga, "Reliable identification schemes for asset and production tracking in industry 4.0," *Sensors*, vol. 20, no. 13, p. 3709, 2020.
- [2] A. Motroni, A. Buffi, and P. Nepa, "Forklift tracking: Industry 4.0 implementation in large-scale warehouses through uwb sensor fusion," *Applied Sciences*, vol. 11, no. 22, p. 10607, 2021.
- [3] N. Macoir, J. Bauwens, B. Jooris, B. Van Herbruggen, J. Rossey, J. Hoebeke, and E. De Poorter, "Uwb localization with battery-powered wireless backbone for drone-based inventory management," *Sensors*, vol. 19, no. 3, p. 467, 2019.
- [4] M. Elsanhoury, P. Mäkelä, J. Koljonen, P. Väliä, A. Shamsuzzoha, T. Mantere, M. Elmusrati, and H. Kuusniemi, "Precision positioning for smart logistics using ultra-wideband technology-based indoor navigation: A review," *IEEE Access*, 2022.
- [5] B. Van Herbruggen, J. Fontaine, and E. De Poorter, "Anchor pair selection for error correction in time difference of arrival (tdoa) ultra wideband (uwb) positioning systems," in *2021 International Conference on Indoor Positioning and Indoor Navigation (IPIN)*. IEEE, 2021, pp. 1–8.
- [6] H. Chen and A. Dhekne, "Pnploc: Uwb based plug & play indoor localization," in *2022 IEEE 12th International Conference on Indoor Positioning and Indoor Navigation (IPIN)*. IEEE, 2022, pp. 1–8.
- [7] S. N. A. Ahmed and Y. Zeng, "Uwb positioning accuracy and enhancements," in *TENCON 2017-2017 IEEE Region 10 Conference*. IEEE, 2017, pp. 634–638.
- [8] IDLab, "Iiot testbed," 2017, (Accessed on 2023-06-19). [Online]. Available: <https://www.ugent.be/ea/idlab/en/research/research-infrastructure/industrial-iiot-lab/html/>
- [9] C. Chen, Z. Huang, J. Wang, L. Yuan, J. Bao, and Z. Chen, "Channel-quality-evaluation-based anchor node selection for uwb indoor positioning," *Electronics*, vol. 11, no. 3, p. 436, 2022.
- [10] A. Courty, M. Le Gentil, O. Berder, P. Scalart, S. Fontaine, and A. Carer, "Anchor selection algorithm for mobile indoor positioning using wsn with uwb radio," in *2019 IEEE Sensors Applications Symposium (SAS)*. IEEE, 2019, pp. 1–5.
- [11] S. Djovic, I. Stojanovic, M. Jovanovic, T. Nikolic, and G. L. Djordjevic, "Fingerprinting-assisted uwb-based localization technique for complex indoor environments," *Expert Systems with Applications*, vol. 167, p. 114188, 2021.
- [12] C. De Cock, S. Coene, B. Van Herbruggen, L. Martens, W. Joseph, and D. Plets, "Imu-aided detection and mitigation of human body shadowing for uwb positioning," in *2022 IEEE 12th International Conference on Indoor Positioning and Indoor Navigation (IPIN)*. IEEE, 2022, pp. 1–8.
- [13] A. R. Jiménez and F. Seco, "Improving the accuracy of decawave's uwb mdek1001 location system by gaining access to multiple ranges," *Sensors*, vol. 21, no. 5, p. 1787, 2021.
- [14] *DWM1001 System Overview And Performance*, Decawave Ltd, 2018, version 2.1.
- [15] F. Che, Q. Z. Ahmed, J. Fontaine, B. Van Herbruggen, A. Shahid, E. De Poorter, and P. I. Lazaridis, "Feature-based generalized gaussian distribution method for nlos detection in ultra-wideband (uwb) indoor positioning system," *IEEE Sensors Journal*, vol. 22, no. 19, pp. 18 726–18 739, 2022.
- [16] *DW1000 Datasheet*, Decawave Ltd, 2017, version 2.22.
- [17] J. A. Shaw, "Radiometry and the friis transmission equation," *American journal of physics*, vol. 81, no. 1, pp. 33–37, 2013.
- [18] Y. Zhang, D. Wei, W. Fu, and B. Yang, "Target positioning with gdop assisted nodes selection algorithm in wireless sensor networks," *International Journal of Distributed Sensor Networks*, vol. 10, no. 6, p. 404812, 2014.
- [19] B. Van Herbruggen, B. Jooris, J. Rossey, M. Ridolfi, N. Macoir, Q. Van den Brande, S. Lemey, and E. De Poorter, "Wi-pos: A low-cost, open source ultra-wideband (uwb) hardware platform with long range sub-ghz backbone," *Sensors*, vol. 19, no. 7, p. 1548, 2019.
- [20] G. Mao, S. Drake, and B. D. Anderson, "Design of an extended kalman filter for uav localization," in *2007 Information, Decision and Control*. IEEE, 2007, pp. 224–229.